Perfluorobutane Sulfonic Acid Hydration and Interactions with O_2 Adsorbed on Pt_3

Liuming Yan,[†] Perla B. Balbuena,*[,†] and Jorge M. Seminario*[,†,‡]

Departments of Chemical Engineering and Electrical Engineering, Texas A&M University, College Station, Texas 77843

Received: November 21, 2005; In Final Form: February 9, 2006

The side chain of NAFION, a proton conductive membrane used as electrolyte in low-temperature fuel cells, is modeled with perfluorobutane sulfonic acid. Density functional theory is used to characterize structures and energetics of hydration of the model system interacting with a proton solvated with up to 24 water molecules and analyze interactions of some of these hydrated complexes with O_2 adsorbed on Pt_3. It is found that at least three water molecules are needed to ionize the sulfonic acid, and higher degrees of hydration induce the formation of cages where the water molecules are held together via complex hydrogen-bond networks. The interaction between the complex formed by the ionized acid and the hydrated proton, in contact with a bridge-adsorbed O_2-Pt_3, promotes the protonation of the adsorbed O_2. Upon protonation, the O_2-Pt_3 system evolves from hydrophobic to hydrophilic behavior, which may facilitate further interfacial contact.

1. Introduction

The high cost and slow kinetics of the catalyzed oxygen reduction reaction are some of the major hindrances for large-scale commercialization of low-temperature proton-exchange membrane (PEM) fuel cells.[1,2] Due to their low platinum loading, relatively high reactivity, and chemical stability, carbon-supported platinum and platinum−alloy nanostructures are currently the best choices for PEM fuel cells oxygen electroreduction catalysts.[3−13] Although the oxygen electroreduction has been well characterized over various electrode surfaces in various electrolytes, disagreements on the detailed mechanism at the molecular level still exist.[14−26] Besides the disagreement on the reaction pathways,[27−31] there is a controversy regarding the first step, usually considered rate determining, of the oxygen reduction on Pt electrodes, which may occur via dissociative adsorption of oxygen followed or preceded by protonation of the adsorbed species in acid medium. We have recently shown that several factors such as the initial O_2-surface and O_2-proton distances and the degree of proton solvation can alter the sequence proton−electron transfer to the O_2 molecule interacting with the catalyst surface.[23,32−34] A proton usually associates with one or two H_2O molecules in bulk liquid water, forming structures such as hydronium $H^+(H_2O)$ and Zundel $H^+(H_2O)_2$ cations;[35] the hydronium ion readily associates with three more water molecules, forming the Eigen cation $H^+(H_2O)_4$.[36] Experimental evidence shows that the Eigen cation is slightly more stable than the Zundel cation by ∼2.4 kJ/mol.[37] These cations would continue to loosely associate with more H_2O molecules, forming complex clusters $H^+(H_2O)_n$. Complex hydronium clusters as large as $H^+(H_2O)_{21}$ have been observed using the photodissociation spectrum in a supersonic free jet expansion vapor.[38−40] In addition, the PEM electrocatalyst is surrounded by a hydrated proton-conductive polymer membrane. Thus, the accessibility of the proton to the vicinity of the catalyst surface where the O_2 molecule should be reduced is dependent on the configuration of the polymeric membrane in contact with the nanocatalyst and on the degree of hydration of such membrane. The most common membrane used for PEM fuel cells is NAFION, a complex fluorinated polymer grafted with sulfonic acid functional groups.[41] Recent reports[42,43] have investigated the hydration and proton transfer in model membrane materials such as CF_3SO_3H, $CH_3C_6H_4SO_3H$, and $CF_3OCF_2CF_2SO_3H$. These studies concluded that dissociation of RSO_3H occurs as a result of delocalization of positive charges in the hydrogen-bonding network of water and negative charges in the sulfonic group and the fluorinated side chain and that the Zundel and Eigen complexes are limiting configurations which may dynamically convert into each other during transfer of protons in PEMs as it does in bulk water.[42] However, the influence on the protonation step exerted by hydronium clusters interacting with the sulfonic acid side chain of NAFION, under different hydration conditions in acid solution, is not well characterized yet.

In this work, the hydration of perfluorobutane sulfonic acid ($PFBSO_3H$), which resembles the sulfonic acid group grafted on NAFION, is studied using first-principles calculations. Various complex hydronium clusters as well as preliminary insights into their effect on the first step of the oxygen reduction are also studied.

2. Computational Details

The chemical structure of NAFION is displayed in Figure 1a. According to the Gierke and Hsu model,[41] dry NAFION membranes arrange forming cavities interconnected by narrow channels; it is estimated that the average cavity has a diameter of ∼1.8 nm and contains ∼26 acid groups.[41] In a hydrated state, the average cavity might be filled with ∼1000 H_2O molecules, its diameter increases to ∼4 nm, the channel diameter and length increase to ∼1 nm,[41] and the number of sulfonic acid groups on the surface of a cavity increases to ∼70 (Figure 1b).[44] Using these data one can estimate that each sulfonic acid group is hydrated by ∼14 water molecules. Recent analyses using small-angle X-ray[45,46] and neutron scattering have provided improved models of ionomers microstructure based on rodlike particles,

* To whom correspondence should be addressed. E-mail: balbuena@tamu.edu, seminario@tamu.edu.
[†] Department of Chemical Engineering.
[‡] Department of Electrical Engineering.

10.1021/jp056748r CCC: $33.50 © 2006 American Chemical Society
Published on Web 03/15/2006

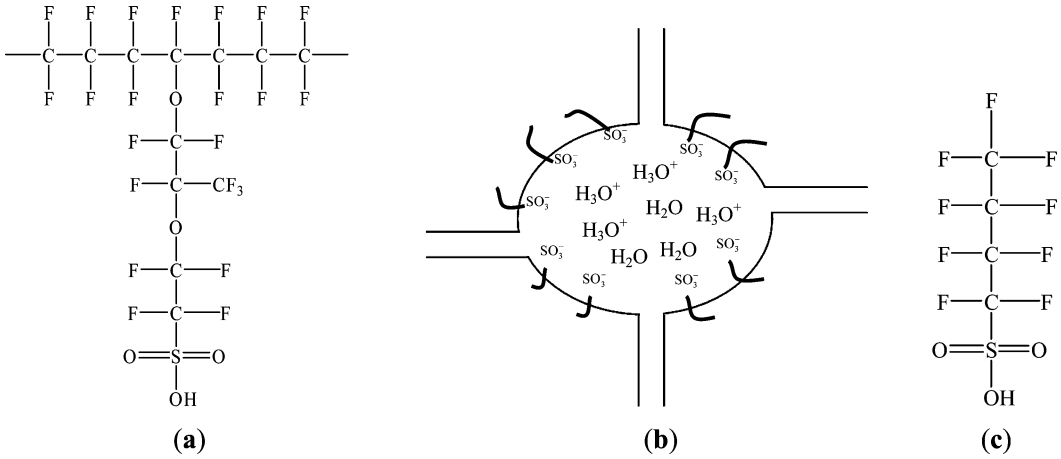

Figure 1. (a) NAFION is a fluorinated polymer grafted with sulfonic acid. (b) The bulk NAFION membrane is a porous material. When hydrated, it is speculated[41] that a typical cavity may be usually ~4 nm diameter connected to other cavities by channels of 1 nm in length and 1 nm in diameter. There are ~70 sulfonic acid (SO_3^-) groups on the surface of each cavity hydrated by ~1000 H_2O molecules. (c) Perfluorobutane sulfonic acid ($PFBSO_3H$) used in this work to emulate the sulfonic acid group of NAFION.

as discussed by Gebel and Diat,[47] and comparative studies of the microstructure of different ionomers were reported by Kreuer's group.[42,48] We selected $PFBSO_3H$, which has a similar structure to the grafted sulfonic acid groups on NAFION (Figure 1c); thus, similarity between $PFBSO_3H$ and the sulfonic acid-terminated side chain on NAFION can be expected.

Theoretical calculations of $(PFBSO_3H)(H_2O)_n$ clusters are based on density functional theory[49−51] as implemented in the GAUSSIAN 03 program.[52] All clusters are optimized using the functional/basis set B3PW91/6-31G(d, p),[53−56] and the optimized geometries are verified to be local minima by second-derivative calculations at the same level of theory.

3. Structural Characteristics of Hydrated $PFBSO_3H$ Clusters

3.1. Nomenclature and Criteria Used for H Bonding and Ionization. Hydrated $PFBSO_3H$ clusters are associated by two types of hydrogen bond: those between H_2O and SO_3 and those between two H_2O molecules. An H bond is defined on the basis of the distance and angle criteria by which a bond is considered formed if an H atom is located between two O atoms that are at a distance ≤ 3.1 Å and the OHO angle is $\geq 145°$.[57] A H_2O molecule that donates (accepts) one H atom to (from) a hydrogen bond is a hydrogen-donor molecule (D-H_2O) (a hydrogen-acceptor molecule (A-H_2O)). A water molecule can accept (donate) at most two H atoms; in that case it is an AA-H_2O (DD-H_2O). It can also simultaneously serve as H acceptor and H donor; this is AD-H_2O, AAD-H_2O, ADD-H_2O, or AADD-H_2O. The O atoms from ionized SO_3 can only serve as H acceptors.

An OH that is related to an H bond is called an H-bonded OH or HB OH, and it is called a non-H-bonded OH or NHB OH if it is not related to any hydrogen bond. A NHB OH usually has a higher stretching frequency than that of HB OH.[39,40]

Ionization is considered to occur when the distance from the nearest H atom to $PFBSO_3^-$ is larger than 1.2 Å, significantly elongated with respect to the OH distance in the undissociated acid (0.972 Å). Our calculations show that $PFBSO_3H$ does not ionize in $(PFBSO_3H)(H_2O)_n$ clusters when $n = 1$ or 2; however, it ionizes in all clusters when $n = 3$ or larger. The OH distance increases to 1.023 and 1.074 Å when $n = 1$ or 2, respectively, and is 1.568 Å in $(PFBSO_3H)(H_2O)_3$; thus, according to our criterion, $PFBSO_3H$ in this case has ionized becoming $(PFBSO_3)^-H^+(H_2O)_3$.

TABLE 1: Structural Characteristics of $(PFBSO_3H)(H_2O)_n$

			OH stretching frequency (cm^{-1})		
n	geometry	complex ion	H_3O^+	HB OH	NHB OH
0					3589
1	4^1			2676−3547	3700
2	5^1			1978−3482	3698−3702
3	5^26^1	$H^+(H_2O)_3$	2349−2782	3228−3261	3693
4	5^4	$H^+(H_2O)_3$	2742−3196	3360−3453	3698−3700
5	5^26^2	$H^+(H_2O)_4$	1743−2839	3108−3457	3692−3709
6	$4^25^28^1$	$H^+(H_2O)_3$	2026	2875−3511	3697−3708
7	$4^25^28^1$	$H^+(H_2O)_3$	1868	3099−3636	3704−3710
8	$4^35^26^2$	$H^+(H_2O)_3$	1795−2093	2918−3584	3705−3714
9	$4^35^26^1$	$H^+(H_2O)_3$	2177	3046−3598	3664−3707
10	$4^45^56^1$	$H^+(H_2O)_4$	2518−2793	3088−3660	3695−3703
11	$3^14^65^16^17^1$	$H^+(H_2O)_3$	2722	2763−3584	3701−3706
12	$4^66^38^1$	$H^+(H_2O)_3$	2046−2414	2664−3644	3696−3706
13	$3^14^65^17^2$	$H^+(H_2O)_4$	2096−2689	2821−3593	3700−3707
14	$3^44^55^17^1$	$H^+(H_2O)_4$	2260−2408	2769−3639	3700−3710
15	$3^14^45^36^4$	$H^+(H_2O)_4$	2079−2305	2611−3583	3690−3707

When a proton associates with one H_2O molecule forming the hydronium ion $H^+(H_2O)$, the H bond formed between H_3O^+ and H_2O usually has a much shorter bond length than those between two neutral H_2O molecules or between SO_3 and H_2O. If a water molecule is close to a hydronium ion with an O−O distance less than 2.5 Å, the molecule is considered to be closely associated with the hydronium ion and loosely associated if the O−O distance is between 2.5 and 2.6 Å. In both cases the hydronium ion and associated water molecules are considered to be part of a complex hydronium ion $H^+(H_2O)_n$.

Picturing an H bond as a line that connects two O atoms, several H bonds can form a closed ring. These rings, in turn, are able to form cage structures by sharing edges and vertexes. A ring is characterized by the number of connected heavy atoms (O and S) and a cage by the number of rings.[58] Therefore, a N^iM^j cage has *i* N-member rings and *j* M-member rings; a 5^26^1 cage has two five-member rings and one six-member ring. In the next section we analyze cage structures associated with $PFBSO_3H$.

3.2. Structures of Hydrated and Free $PFBSO_3H$ Clusters. Evaluating the effect of membrane hydration on the PEM fuel cell performance, researchers define a parameter λ as the ratio of the number of water molecules to the number of sulfonic acid groups, and it is found that the optimum value of λ associated with high proton conductivity ranges between 15 and 20.[43] Here we examine the structure of $PFBSO_3H$ interacting with hydrated protons forming complex cage structures corre-

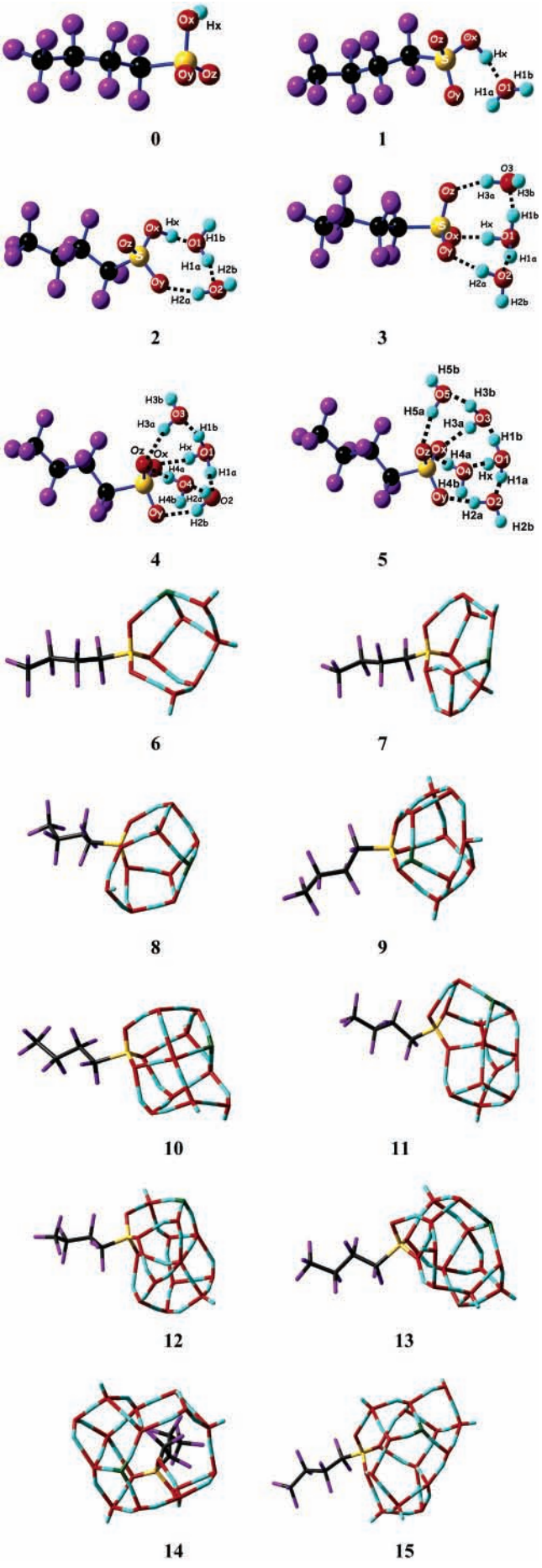

Figure 2. Structures and atom labeling of hydrated $PFBSO_3H$ clusters

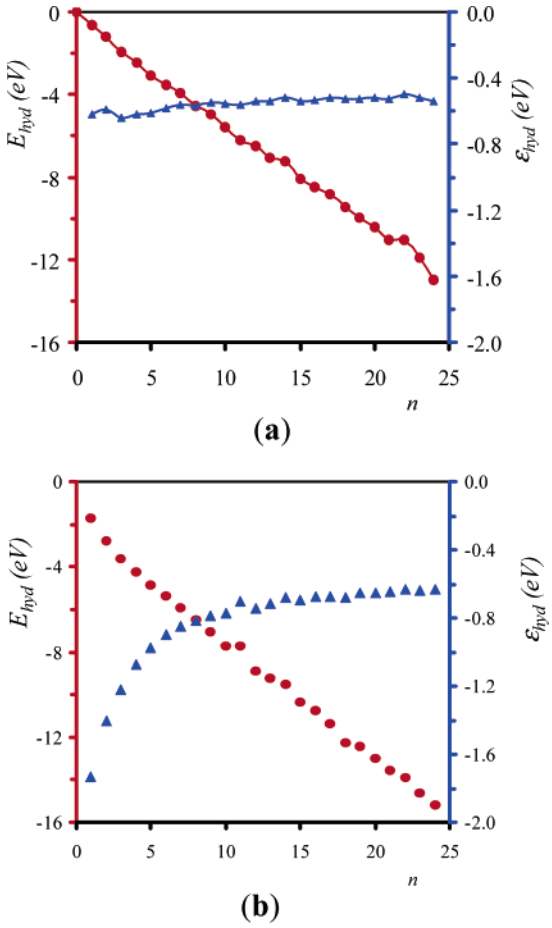

Figure 3. Total hydration energy E_{hyd} (solid circle) and average hydration energy contributed from each water molecule ϵ_{hyd} (solid triangle) of (a) $(PFBSO_3)^-H^+(H_2O)_n$ cluster and (b) protonated $H^+(H_2O)_n$ cluster.

sponding to λ values from 0 to 15 as indicated in Table 1 and Figure 2. The most relevant geometric characteristics of these structures can be summarized as follows. The atom labeling used in this section is indicated in Figure 2.

0. Free $PFBSO_3H$. Relevant bond lengths are as follows: Ox−Hx, 0.972 Å; S−Ox, 1.619 Å; S−C, 1.878 Å; S−Oy and S−Oz, 1.452 and 1.444 Å, respectively; C−F 1.332−1.350 Å; C−C, 1.551−1.555 Å.

1. $(PFBSO_3H)(H_2O)$: $PFBSO_3H$ is not ionized. The Ox−Hx bond length (1.023 Å) is much shorter than the distance between the H atom and the nearest water O1 atom of 1.563 Å (O1−Hx). The S−Ox bond length (1.583 Å) is longer than that of free $PFBSO_3H$. The S−Oy and S−Oz distances are 1.446 and 1.464 Å, respectively. The OH vibrational frequency of the sulfonic group decreases to 2676 cm^{-1}. The symmetric and asymmetric OH stretching modes of water are 3547 and 3700 cm^{-1}.

2. $(PFBSO_3H)(H_2O)_2$. Two water molecules and the SO_3 group form a five-member ring, where $PFBSO_3H$ is not ionized; the Ox−Hx bond length is 1.074 Å, which is shorter than the distance between the H atom and the nearest water O atom of 1.390 Å (O1−Hx). The S−Ox, S−Oy, and S−Oz bond lengths are 1.557, 1.468, and 1.448 Å, respectively. The OH stretching frequency in $PFBSO_3H$ decreases to 1978 cm^{-1}. The stretching frequency of the OH which connects to a sulfonic O is 3482 cm^{-1}, and the HB OH stretching frequency is 3015 cm^{-1}.

3. $(PFBSO_3H)(H_2O)_3$ or $(PFBSO_3)^-H^+(H_2O)_3$, In these clusters $PFBSO_3H$ is ionized with a cage structure of 5^26^1. The

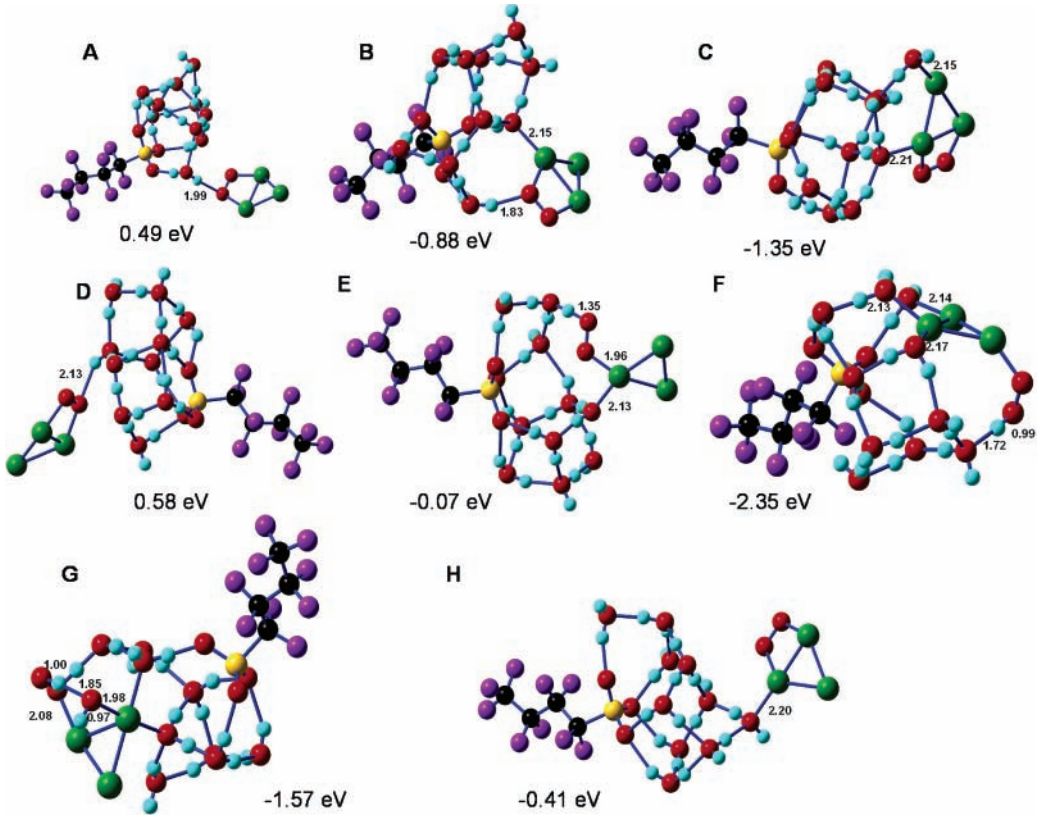

Figure 4. Local minima configurations of the combined system of a $(PFBSO_3)^-H^+(H_2O)_{10}$ cluster interacting with a bridge-adsorbed O_2-Pt_3 cluster. The association energies are calculated from the energy difference between the complex and the separated $(PFBSO_3)^-H^+(H_2O)_{10}$ and bridge-adsorbed O_2-Pt_3.

distance from $PFBSO_3$ to the nearest H atom (Ox−Hx) is 1.568 Å; this is much longer than the OH bond length in H_3O^+ of 1.021 Å (O1−Hx). The other two water molecules form an H bond with the O atom in $(PFBSO_3)^-$; and the Oy−H2a and Oz−H3a distances are 1.741 and 1.761 Å, respectively. The S−Ox, S−Oy, and S−Oz bond lengths are 1.496, 1.483, and 1.480 Å. The OH stretching frequencies in $H^+(H_2O)$ are 2349, 2464, and 2782 cm^{-1}.

4. $(PFBSO_3)^-H^+(H_2O)_4$. $PFBSO_3H$ is ionized with a cage structure of 5^4. The OH bond lengths in $H^+(H_2O)$ (designated as O1−Hx, O1−H1a, and O1−H1b) are 0.993, 1.135, and 1.020 Å. The OH distances from an H atom in H_3O^+ to its nearest O atoms (O2−H1a, O3−H1b, and Ox−Hx) are 1.302, 1.570, and 1.751 Å, respectively. The OH stretching frequencies of $H^+(H_2O)$ are 2742, 2991, and 3196 cm^{-1}; the HB OH stretching frequencies are 3360, 3416, and 3453 cm^{-1}; the two NHB OH stretching frequencies are 3698 and 3700 cm^{-1}.

5. $(PFBSO_3)^-H^+(H_2O)_5$. $PFBSO_3H$ is ionized with 5^26^2 cage structure. The OH bond lengths in $H^+(H_2O)$ (O1−H1a, O1−Hx, and O1−H1b) are 1.015, 1.017, and 1.098 Å, respectively. The H-bond lengths between $H^+(H_2O)$ and the water molecules (O3−H1b, O2−H1a, and O4−Hx) are 1.352, 1.568, and 1.572 Å. The OH stretching frequencies in H_3O^+ are from 1743 to 2893 cm^{-1}, the HB OH stretching frequencies range from 3108 to 3457 cm^{-1}, and the NHB OH stretching frequencies are 3692−709 cm^{-1}.

6. $(PFBSO_3)^-H^+(H_2O)_6$. $PFBSO_3H$ is ionized with $4^25^28^1$ cage structure. The OH bond lengths in $H^+(H_2O)$ (O1−Hx, O1−H1a, and O1−H1b) are 1.012, 1.068, and 1.026 Å, respectively. The lowest OH stretching frequency is 2026 cm^{-1}, the HB OH stretching range is from 2875 to 3511 cm^{-1}, and the three NHB OH stretching frequencies are in the range 3697−3708 cm^{-1}.

4. Mulliken Charge Distribution

In free $PFBSO_3H$, both the SO_3 and perfluorobutyl groups are negatively charged with −0.27 *e* and −0.11 *e* (where *e* is the elementary charge) due to the strong electron affinity characteristic of both the F atom and the SO_3 group and the H atom is positively charged with 0.38 *e*. In $(PFBSO_3H)(H_2O)_n$ ($n = 1, 2$) cluster, where the H atom of $PFBSO_3H$ is not ionized, the charge on SO_3 increases to −0.38 *e* and −0.43 *e* for $n = 1$ and 2, respectively, and the H atom of $PFBSO_3H$ has a positive charge of 0.42 *e* and 0.45 *e*. In $(PFBSO_3)^-H^+(H_2O)_n$ ($n \geq 3$) cluster, where the H atom of $PFBSO_3H$ is ionized and the cation and anion are well separated, the $(PFBSO_3)^-$ bears −0.78 *e* with −0.63 *e* on the SO_3 group, much lower values than those corresponding to the stoichiometric charge. The complex of the hydronium ion including all the water molecules bears 0.78 *e*, and the $H^+(H_2O)$ itself bears 0.59 *e*. The charge on perfluorobutyl is almost unaffected by hydration, ranging from −0.11 to −0.17 *e* for $n = 0-24$. From these calculations we can conclude that the positive (or negative) charges are delocalized in the hydrogen-bonding network (or fluorinated butyl and sulfonic group) and the ionized states are stabilized; these results are consistent with other calculations,[43] although the entropic term which may contribute to the stabilization of these states is not included.

5. Hydration and Ionization Energy of $PFBSO_3H$

The hydration energy $E_{hyd}(PFBSO_3H)$ is calculated as the total energy difference between products and reactants for the reaction

$$PFBSO_3H + nH_2O \rightarrow (PFBSO_3)^-H^+(H_2O)_n \qquad (1)$$

corrected with the zero-point energy. The zero-point energy is

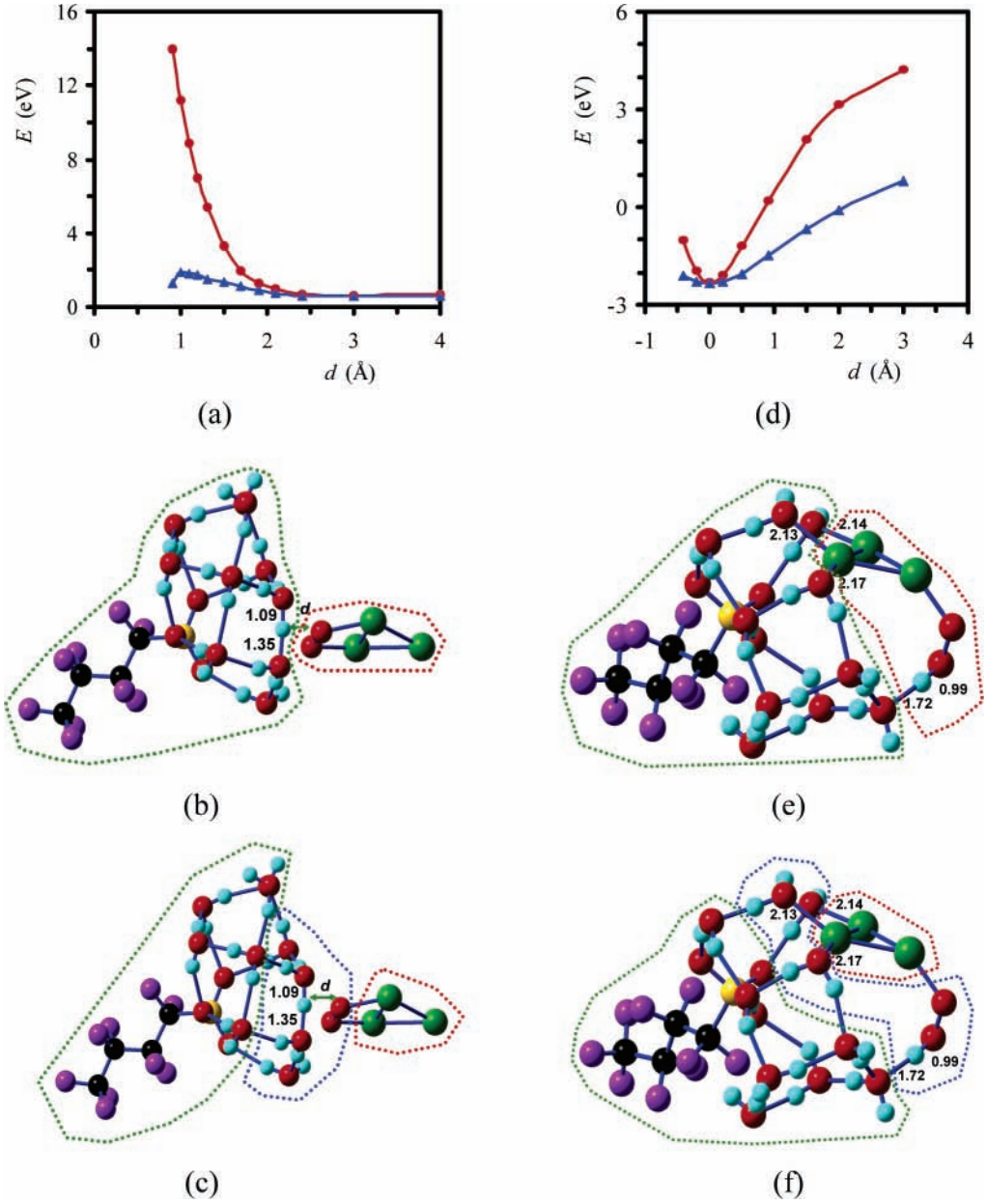

Figure 5. Interaction energies between $(PFBSO_3)^-H^+(H_2O)_{10}$ and O_2-Pt_3 and between $(PFBSO_3)(H_2O)_{10}$ and the on-top protonated $HOO-Pt_3$. (a) The association energy (red, solid circle) between $(PFBSO_3)^-H^+(H_2O)_{10}$ and O_2-Pt_3 is always positive (hydrophobic) and monotonically increases when the separation between the two groups decreases: the two groups are enclosed by the red and green dotted curves in configuration b. Repulsive association energies are found (blue, solid triangle) even if a few water molecules, enclosed by the blue dotted curve, located at the interface between the two clusters, rearrange to minimize the association energy with the bridge-adsorbed O_2 as shown in configuration c, whereas the atoms from the other two groups, enclosed by the green and red dotted curves, are held fixed as the distance *d* changes. (d) The association energy (red, solid circle) between $(PFBSO_3)(H_2O)_{10}$ and the on-top protonated $HOO-Pt_3$ cluster shows a deep well (hydrophilic) when the separation between the two groups changes while the atoms in each group are held fixed; the two groups are enclosed by the red and green dotted curves in configuration e. The potential well becomes more shallow (blue, solid triangle in d) when a few water molecules and the on-top protonated HOO at the interface between the two clusters, highlighted by the blue dotted curve in configuration f, are rearranged to minimize the association energy while the atoms of the other two groups, highlighted by the red and green dotted curves in configuration f, are held fixed as the distance *d* changes.

calculated by summing the zero-point energies of all harmonic vibration modes in the cluster. The calculated harmonic vibrational frequency is usually slightly larger than the experimental IR or Raman frequency due to the anharmonic nature of the vibrational mode. It has been reported in several experiments that the stretching frequency of a NHB OH in a AAD-H_2O in protonated H_2O cluster is $\sim$3695 cm^{-1}.[39,40,58] Our calculations for protonated H_2O clusters show an average stretching frequency for the corresponding NBH OH of 3890 cm^{-1}. Thus, a scaling factor of 0.947, which is the ratio of the experimental IR frequency of the NHB OH stretching mode to the calculated frequency of the corresponding vibrational mode in a protonated water cluster,[59] is applied to all the calculated frequencies. The reason for using the scaling factor of the protonated H_2O cluster instead of that of $(PFBSO_3)^-H^+(H_2O)_n$ itself is due to the lack of experimental information on $(PFBSO_3)^-H^+(H_2O)_n$ clusters, and the similarity of the protonated H_2O part between these two systems suggests closeness between their scaling factors. A comparison between the hydration energy of $H^+(H_2O)$ and $PFBSO_3H$ is also made. The hydration energy $E_{hyd}(H^+(H_2O))$ is calculated from

$$(n-1)H_2O + H^+(H_2O) \rightarrow H^+(H_2O)_n \qquad (2)$$

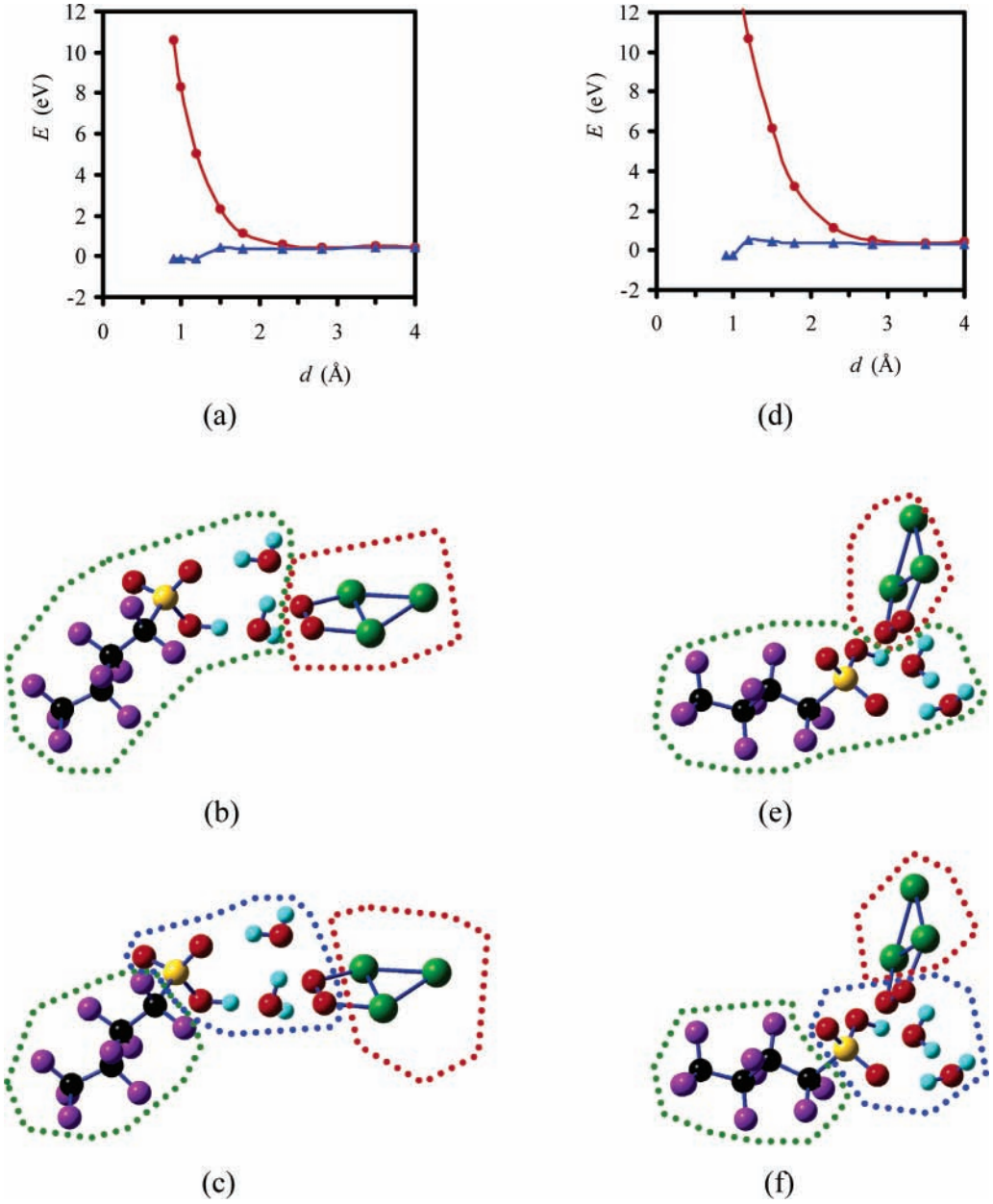

Figure 6. Association energy between the bridge-adsorbed O_2-Pt_3 cluster and $(PFBSO_3H)(H_2O)_2$ where ionization does not occur is always repulsive. (a) The association energy (red, solid circle) increases monotonically as their separation decreases, as shown in configuration b, where the two groups enclosed by the blue and red dotted curves are held fixed while the distance *d* between them changes, or slightly decreases (blue, solid triangle) as *d* decreases in configuration c, where only the atoms at the interface enclosed by the blue dotted curve are allowed to rearrange to decrease the energy. (d) Similar association energy is predicted for configurations e and f, where the bridge-adsorbed O_2 is close to the acidic hydrogen of $PFBSO_3H$. The red solid circles correspond to configuration e, where the separation *d* between the two groups changes, and the blue solid triangles correspond to configuration f, where the separation between the two groups enclosed by the red and blue dotted curves changes whereas the atoms inside the blue dotted curve rearrange to minimize the total energy.

corrected by the zero-point energy scaled with the same scaling factor as that of $(PFBSO_3)^-H^+(H_2O)_n$ cluster.

The calculated hydration energy increases as more water molecules are added to the cluster (Figure 3). The average hydration energy contributed from each water molecule is evaluated as

$$\epsilon_{hyd} = E_{hyd}/n \tag{3}$$

for the $(PFBSO_3)^-H^+(H_2O)_n$ cluster or

$$\epsilon_{hyd} = E_{hyd}/(n-1) \tag{3'}$$

for the $H^+(H_2O)_n$ cluster. Notice the difference between these two formulas: the average hydration energy for the $(PFBSO_3)^-H^+(H_2O)_n$ clusters is an energy averaged with *n* water molecules, while the average hydration energy for the $H^+(H_2O)_n$ clusters is averaged with $n-1$ since we are dealing with the hydration of $H^+(H_2O)$ not H^+. For the protonated water cluster ϵ_{hyd} decreases rapidly with the increase of *n* for $n < 10$; however, the ϵ_{hyd} value gradually saturates as *n* increases. The saturated ϵ_{hyd} for the protonated H_2O cluster is ~ -0.63 eV. For the $(PFBSO_3)^-H^+(H_2O)_n$ cluster the change of ϵ_{hyd} versus the number of water molecules is not as significant as in the protonated H_2O cluster. ϵ_{hyd} only slightly decreases from ~ -0.6 eV to ~ -0.52 eV when *n* increases from 1 to 24.

In a vacuum the hydrogen ionization energy of $PFBSO_3H$

$$PFBSO_3H \rightarrow (PFBSO_3)^- + H^+ \quad (4)$$

is 13.34 eV. However, the ionization energy in solvent includes the Coulomb interaction between $(PFBSO_3)^-$ and H^+ since these two ions are not infinitely separated. Assuming that SO_3 and $H^+(H_2O)$ are point charges bearing average Mulliken charges of -0.6 and 0.6 *e* (as described in section 4) and their separation distance is 1.6 Å in the ionized state, the Coulomb interaction is -3.24 eV if the effect from the media permittivity is neglected. Thus, the ionization energy of $PFBSO_3H$ in solvent is ~10.10 eV. The calculated formation energy of $H^+(H_2O)$, -7.49 eV, is lower than the energy needed for the ionization of $PFBSO_3H$; therefore, ionization is impossible with only one water molecule. However, the ionization energy can be compensated by the hydration energy of additional water molecules. For example, the hydration energy of $H^+(H_2O)_3$ is -2.80 eV, which is enough to compensate for the ionization energy of $PFBSO_3H$. Further insights may be gained from calculation of chemical potentials on the basis of calculated hydration enthalpies and entropies and comparison to experimental data from hydration isotherms.[43]

6. Oxygen Adsorption on Pt_3 in the Presence of Hydrated $PFBSO_3H$

6.1. Interaction between $(PFBSO_3)^-H^+(H_2O)_{10}$ and Bridge-Adsorbed O_2-Pt_3. Several stable configurations and association energies of the combined system of $(PFBSO_3)^-H^+(H_2O)_{10}$ and a bridge-adsorbed O_2-Pt_3 cluster optimized from various starting configurations using density functional theory are shown in Figure 4. The association energy is calculated as the energy difference between the total energy of the complex and the sum of the total energies of the separated components. It is found that the $(PFBSO_3)^-H^+(H_2O)_{10}$ cluster repels (based on the positive associating energy of 0.5 eV) the bridge-adsorbed O_2-Pt_3 cluster when the interaction at the interface is only between O_2 and water (configurations **A** and **D**). On the other hand, the $(PFBSO_3)^-H^+(H_2O)_{10}$ cluster does attract (negative association energy) the bridge-adsorbed O_2-Pt_3 cluster when the Pt_3 side interacts with the water molecules of the $(PFBSO_3)^-H^+(H_2O)_{10}$ cluster (configurations **B**, **C**, and **H**). In configurations **F** and **G** the adsorbed O_2 is readily protonated, forming on-top adsorbed OOH; it is found that the protonated configurations are more stable than the nonprotonated configurations. The adsorption of a water molecule on the Pt atom where the protonated oxygen is adsorbed decreases the stability of the Pt−OOH bond, thus easing the desorption of OOH (configuration **E**).

Because of the interaction of $(PFBSO_3)^-H^+(H_2O)_{10}$ and bridge-adsorbed O_2-Pt_3, the water affinity of Pt_3 in contact with O_2 changes from a hydrophobic to a hydrophilic state after the adsorbed O_2 is protonated. The hydrophobicity of Pt_3 in contact with a bridge-adsorbed O_2 is inferred from the association energy between a $(PFBSO_3)^-H^+(H_2O)_{10}$ cluster and a bridge-adsorbed O_2-Pt_3 cluster (Figure 5a), where the association energy between these two components is shown as a function of the distance separating them (Figure 5b and c). The bridge-adsorbed O_2 changes to end-on adsorption if the geometry optimization starts with an initial guess value *d* smaller than 1.2 Å (Figure 5c); however, if the initial guess distance *d* is greater than 1.2 Å, the change is not observed. The optimized O−O bond length shortens to 1.265 Å starting from an initial distance $d = 0.9$ Å, but even with such an unrealistically short initial distance protonation of the adsorbed O_2 does not occur under these conditions. The optimized O−O bond length from the adsorbed O_2 slightly varies from 1.315 to 1.326 Å for cases when the guess distance *d* is in the range from 1.0 to 4.0 Å. The changes in charge on O atoms are not significant either as the Mulliken population of O atoms varies from -0.2 to -0.3. On the other hand, attractive energies are found between the on-top $HOO-Pt_3$ and the hydrated $(PFBSO_3)^-H^+(H_2O)_{10}$ cluster (Figure 5d−f). However, no significant changes in O−O bond lengths or charges on the O atoms are observed regardless of the initial value used for the distance *d* during the geometry optimization (Figure 5f).

6.2 Interaction between $(PFBSO_3H)(H_2O)_2$ and a Bridge-Adsorbed O_2-Pt_3 Cluster. Protonation of the bridge-adsorbed O_2-Pt_3 cluster does not occur if a $PFBSO_3H$ is only hydrated with two water molecules. The proton hydration can compensate for the energy requirement of the ionization of $PFBSO_3H$ (section 5). Direct protonation where a proton transfers directly from the $PFBSO_3H$ to the bridge-adsorbed O_2-Pt_3 cluster was never found. Figure 6 shows that the association energy between the bridge-adsorbed O_2-Pt_3 cluster and the $(PFBSO_3H)(H_2O)_2$ cluster is always repulsive for the various configurations.

7. Conclusions

Ionization of $PFBSO_3H$ occurs only after three or more water molecules hydrate the acid. The ionization energy is compensated by the energy of proton hydration. Hydrated $PFBSO_3H$ clusters arrange in cage-like structures with the water molecules and the SO_3 group associated by multiple hydrogen bonds. The ionization of $PFBSO_3H$ and proton hydration promote the protonation of bridge-adsorbed O_2-Pt_3. However, protonation does not occur if $PFBSO_3H$ is not ionized. In the process of protonation a bridge-adsorbed O_2-Pt_3 complex evolves from hydrophobic to hydrophilic behavior. The bridge-adsorbed O_2-Pt_3 is highly hydrophobic, while the protonated O_2 is hydrophilic. Although these calculations include internal local fields, they do not include the presence of external electric fields; further studies are being carried out to include full effects.

Acknowledgment. Financial support from the Department of Energy Basic Energy Sciences (DE-FG02-05ER15729) is gratefully acknowledged.

References and Notes

(1) Bagotskii, V. S.; Tarasevich, M. R.; Filinovskii, V. Y. *Elektrokhimiya* **1972**, *8*, 84.

(2) Bagotskii, V. S.; Tarasevich, M. R.; Filinovskii, V. Y. Calculation of the Kinetic Parameters of Conjugated Reactions of Oxygen and Hydrogen Peroxide. *Elektrokhimiya* **1969**, *5*, 1218.

(3) Srinivasan, S.; Ticianelli, E. A.; Derouin, C. R.; Redondo, A. Advances in solid polymer electrolyte fuel cell technology with low platinum loading electrodes. *J. Power Sources* **1988**, *22*, 359−375.

(4) Paganin, V. A.; Ticianelli, E. A.; Gonzalez, C. Development and electrochemical studies of gas diffusion electrodes for polymer electrolyte fuel cells. *J. Appl. Electrochem.* **1996**, *26*, 297−304.

(5) Ticianelli, E. A.; Derouin, C. R.; Redondo, A.; Srinivason, S. Methods to advance technology of proton exchange membrane fuel cells. *J. Electrochem. Soc.* **1988**, *135*, 2209−2214.

(6) Passalacqua, E.; Lufrano, F.; Squadrito, G.; Patti, A.; Giorgi, L. Influence of the structure in low-Pt loading electrodes for polymer electrolyte fuel cells. *Electrochim. Acta* **1998**, *43*, 3665−3673.

(7) Jordan, L. R.; Shukla, A. K.; Behrsing, T.; Avery, N. R.; Muddle, B. C.; Forsyth, M. Effect of diffusion-layer morphology on the performance of polymer electrolyte fuel cells operating at atmospheric pressure. *J. Appl. Electrochem.* **2000**, *30*, 641.

(8) Abaoud, H. A.; Ghouse, M.; Lovell, K. V.; Al-Motairy, G. N. A hybrid technique for fabricating PEMFC's low platinum loading electrodes. *Int. J. Hydrogen Energy* **2005**, *30*, 385−391.

(9) Schmidt, T. J.; Paulus, U. A.; Gasteiger, H. A.; Behm, R. J. The Oxygen Reduction Reaction on a Pt/Carbon Fuel Cell Catalyst in the Presence of Chloride Anions *J. Electroanal. Chem.* **2001**, *508* 41−47.

(10) Yang, H.; Vogel, W.; Lamy, C.; Alonso-Vante, N. Structure and electrocatalytic activity of carbon-supported Pt−Ni alloy nanoparticles toward the oxygen reduction reaction. *J. Phys. Chem. B* **2004**, *108*, 11024−11034.

(11) Antolini, E.; Salgado, J. R. C.; Giz, M. J.; Gonzalez, E. R. Effects of geometric and electronic factors on ORR activity of carbon supported Pt−Co electrocatalysts in PEM fuel cells. *Int. J. Hydrogen Energy* **2005**, *30*, 1213−1220.

(12) Ye, S.; Vijh, A. K. Cobalt-carbonized aerogel nanocomposites electrocatalysts for the oxygen reduction reaction. *Int. J. Hydrogen Energy* **2005**, *30*, 1011−1015.

(13) Xiong, L.; Manthiram, A. High performance membrane-electrode assemblies with ultra-low Pt loading for proton exchange membrane fuel cells. *Electrochim. Acta* **2005**, *50*, 3200−3204.

(14) Damjanovic, A.; Brusic, V. Electrode kinetics of oxygen reduction on oxide-free platinum electrodes. *Electrochim. Acta* **1967**, *12*, 615−628.

(15) Damjanovic, A.; Sepa, D. B.; Vojnovic, M. V. New evidence supports the proposed mechanism for O2 reduction at oxide free platinum electrodes *Electrochim. Acta* **1979**, *24*, 887−889.

(16) Yeager, E.; Razaq, M.; Gervasio, D.; Razaq, A.; Tryk, D. Oxygen Reduction in Various Acid Electrolytes *J. Serb. Chem. Soc.* **1992**, *57*, 819−833.

(17) Yeager, E. Electrocatalysts for O2 reduction. *Electrochim. Acta* **1984**, *29*, 1527−1537.

(18) Nolan, P. D.; Lutz, B. R.; Tanaka, P. L.; Davis, J. E.; Mullins, C. B. Molecularly chemisorbed intermediates to oxygen adsorption on Pt-(111): A molecular beam and electron energy-loss spectroscopy study. *J. Chem. Phys.* **1999**, *111*, 3696−3704.

(19) Luntz, A. C.; Williams, M. D.; Bethune, D. S. The sticking of O2 on a Pt(111) surface. *J. Chem. Phys.* **1988**, *89*, 4381−4395.

(20) Sidik, R. A.; Anderson, A. B. Density functional theory study of O2 electroreduction when bonded to a Pt dual site. *J. Electroanal. Chem.* **2002**, *528*, 69−76.

(21) Seminario, J. M.; Agapito, L. A.; Yan, L.; Balbuena, P. B. Density functional theory study of adsorption of OOH on Pt-based bimetallic clusters alloyed with Cr, Co, and Ni. *Chem. Phys. Lett.* **2005**, *410*, 275−281.

(22) Li, T.; Balbuena, P. B. Oxygen reduction on a platinum cluster. *Chem. Phys. Lett.* **2003**, *367*, 439−447.

(23) Wang, X.; Balbuena, P. B. Roles of Proton and Electric Field in the Electroreduction of O2 on Pt(111) Surfaces: Results of an Ab-Initio Molecular Dynamics Study. *J. Phys. Chem. B* **2004**, *108*, 4376−4384.

(24) Markovic, N. M.; Ross, P. N. Electrocatalysis at well-defined surfaces: Kinetics of oxygen reduction and hydrogen oxidation/evolution on Pt(hkl) electrodes. In *Interfacial Electrochemistry. Theory, Experiment and Applications*; Wieckowski, A., Ed.; Marcel Dekker: New York, 1999; pp 821−841.

(25) Adzic, R. R.; Wang, J. X. Configuration and Site of O2 Adsorption on the Pt(111) Electrode Surface. *J. Phys. B* **1998**, *102*, 8988−8993.

(26) Balbuena, P. B.; Altomare, D.; Agapito, L. A.; Seminario, J. M. Theoretical Analysis of Oxygen Adsorption on Pt-Based Clusters Alloyed with Co, Ni, or Cr Embedded in a Pt Matrix. *J. Phys. Chem. B* **2003**, *107*, 13671−13680.

(27) Damjanovic, A.; Genshaw, M. A.; Bockris, J. O. M. Distinction between Intermediates Produced in Main and Side Electrodic Reactions. *J. Chem. Phys.* **1966**, *45*, 4057−4059.

(28) Wroblowa, H. S.; Pan, Y. C.; Razumney, G. Electroreduction of oxygen a new mechanistic criterion. *J. Electroanal. Chem.* **1976**, *69*, 195−201.

(29) Appleby, A. J.; Savy, M. Kinetic of oxygen reduction reactions involving catalytic decomposition of hydrogen peroxide Application to porous and rotating ring-disk electrodes. *J. Electroanal. Chem.* **1978**, *92*, 15−30.

(30) Zurilla, R. W.; Sen, R. K.; Yeager, E. Kinetics of Oxygen Reduction Reaction on Gold in Alkaline-Solution. *J. Electrochem. Soc.* **1978**, *125*, 1103−1109.

(31) Bagotskii, V. S.; Tarasevich, M. R.; Filinovskii, V. Y. *Elektrokhimiya* **1978**, *5*, 1218.

(32) Wang, Y.; Balbuena, P. B. Design of Oxygen Reduction Bimetallic Catalysts: Ab-Initio-Derived Thermodynamic Guidelines. *J. Phys. Chem. B* **2005**, *109*, 18902−18906.

(33) Wang, Y.; Balbuena, P. B. Ab Initio Molecular Dynamics Simulations of the Oxygen Reduction Reaction on a Pt(111) Surface in the Presence of Hydrated Hydronium (H3O)+(H2O)2: Direct or Series Pathway? *J. Phys. Chem. B* **2005**, *109*, 14896−14907.

(34) Wang, Y.; Balbuena, P. B. Potential Energy Surface Profile of the Oxygen Reduction Reaction on a Pt Cluster: Adsorption and Decomposition of OOH and H2O2. *J. Chem. Theory Comput.* **2005**, *1*, 935−943.

(35) Zundel, G.; Metzger, H. Energiebänder der tunnelnden Übershuss-Protenon in flüssigen Säuren. Eine IR-spektroskopische Untersuchung der Natur der Gruppierungen H5O2+. *Z. Phys. Chem.* **1968**, *58*, 225−245.

(36) Eigen, M. Proton-transfer acid−base catalysis + enzymatic hydrolysis. I. elementary processes. *Angew. Chem., Int. Ed. Engl.* **1964**, *3*, 1.

(37) Agmon, N. Proton solvation and proton mobility. *Isr. J. Chem.* **1999**, *39*, 493−502.

(38) Searcy, J. Q.; Fenn, J. B. Clustering of water on hydrated protons in a supersonic free jet expansion. *J. Chem. Phys.* **1974**, *61*, 5282−5288.

(39) Shin, J.-W.; Hammer, N. I.; Diken, E. G.; Johnson, M. A.; Walters, R. S.; Jaeger, T. D.; Duncan, M. A.; Christie, R. A.; Jordan, K. D. Infrared Signature of Structures Associated with the H+(H2O)n (n = 6 to 27) Clusters. *Science* **2004**, *304*, 1137−1140.

(40) Miyazaki, M.; Fujii, A.; Ebata, T.; Mikami, N. Infrared Spectroscopic Evidence for Protonated Water Clusters Forming Nanoscale Cages. *Science* **2004**, *304*, 1134−1137.

(41) Gierke, T. D.; Hsu, W. Y. Perfluorinated ion exchange membranes. In *Perfluorinated Ionomer Membranes*; Eisenberg, A., Yeager, H. L., Eds.; American Chemical Society: Washington, DC, 1982; Vol. 180, pp 283−307.

(42) Kreuer, K.-D.; Paddison, S. J.; Spohr, E.; Schuster, M. Transport in Proton Conductors for Fuel-Cell Applications: Simulations, Elementary Reactions, and Phenomenology. *Chem. Rev.* **2004**, *104*, 4637−4678.

(43) Paddison, S. J. Proton conduction mechanisms at low degrees of hydration in sulfonic acid-based polymer electrolyte membranes. *Annu. Rev. Mater. Res.* **2003**, *33*, 289−319.

(44) Smitha, B.; Sridhar, S.; Khan, A. A. Solid polymer electrolyte membranes for fuel cell applications—a review. *J. Membr. Sci.* **2005**, *259*, 10−26.

(45) Elliott, J. A.; Hanna, S.; Elliott, A. M. S.; Cooley, G. E. Interpretation of the Small-Angle X-ray Scattering from Swollen and Oriented Perfluorinated Ionomer Membranes. *Macromolecules* **2000**, *33*, 4161−4171.

(46) James, P. J.; Elliott, J. A.; McMaster, T. J.; Newton, J. M.; Elliott, A. M. S.; Hanna, S.; Miles, M. J. Hydration of Nafion studied by AFM and X-ray scattering. *J. Mater. Sci.* **2000**, *35*, 5111−5119.

(47) Gebel, G.; Diat, O. Neutron and X-ray Scattering: Suitable Tools for Studying Ionomer Membranes. *Fuel Cells* **2005**, *5*, 261−276.

(48) Kreuer, K. D.; Ise, M.; Fuchs, A.; Maier, J. Proton and water transport in nano-separated polymer membranes. *J. Phys. IV* **2000**, *10*, 279−281.

(49) Hohenberg, P.; Kohn, W. Inhomogeneous Electron Gas. *Phys. Rev. B* **1964**, *136*, 864−871.

(50) Kohn, W.; Sham, L. J. Self-Consistent Equations Including Exchange and Correlation Effects. *Phys. Rev.* **1965**, *140*, A1133−A1138.

(51) Sham, L. J.; Kohn, W. One-Particle Properties of an Inhomogeneous Interacting Electron Gas. *Phys. Rev.* **1966**, *145*, 561−567.

(52) Frisch, M. J.; Trucks, G. W.; Schlegel, H. B.; Scuseria, G. E.; Robb, M. A.; Cheeseman, J. R.; Montgomery, J. A.; Vreven, T., Jr.; Kudin, K. N.; Burant, J. C.; Millam, J. M.; Iyengar, S. S.; Tomasi, J.; Barone, V.; Mennucci, B.; Cossi, M.; Scalmani, G.; Rega, N.; Petersson, G. A.; Nakatsuji, H.; Hada, M.; Ehara, M.; Toyota, K.; Fukuda, R.; Hasegawa, J.; Ishida, M.; Nakajima, T.; Honda, Y.; Kitao, O.; Nakai, H.; Klene, M.; Li, X.; Knox, J. E.; Hratchian, H. P.; Cross, J. B.; Adamo, C.; Jaramillo, J.; Gomperts, R.; Stratmann, R. E.; Yazyev, O.; Austin, A. J.; Cammi, R.; Pomelli, C.; Ochterski, J. W.; Ayala, P. Y.; Morokuma, K.; Voth, G. A.; Salvador, P.; Dannenberg, J. J.; Zakrzewski, V. G.; Dapprich, S.; Daniels, A. D.; Strain, M. C.; Farkas, O.; Malick, D. K.; Rabuck, A. D.; Raghavachari, K.; Foresman, J. B.; Ortiz, J. V.; Cui, Q.; Baboul, A. G.; Clifford, S.; Cioslowski, J.; Stefanov, B. B.; Liu, G.; Liashenko, A.; Piskorz, P.; Komaromi, I.; Martin, R. L.; Fox, D. J.; Keith, T.; Al-Laham, M. A.; Peng, C. Y.; Nanayakkara, A.; Challacombe, M.; Gill, P. M. W.; Johnson, B.; Chen, W.; Wong, M. W.; Gonzalez, C.; Pople, J. A. *Gaussian-2003*, Revision B.4; Gaussian, Inc.: Pittsburgh, PA, 2003.

(53) Becke, A. D. Density-functional thermochemistry. III. The role of exact exchange. *J. Chem. Phys.* **1993**, *98*, 5648−5652.

(54) Perdew, J. P.; Chevary, J. A.; Vosko, S. H.; Jackson, K. A.; Pederson, M. R.; Singh, D. J.; Fiolhais, C. Atoms, molecules, solids, and surfaces: Applications of the generalized gradient approximation for exchange and correlation. *Phys. Rev. B* **1992**, *46*, 6671−6687.

(55) Perdew, J. P.; Wang, Y. Accurate and simple analytic representation of the electron-gas correlation energy. *Phys. Rev. B* **1992**, *45*, 13244−13249.

(56) Frisch, M. J.; Pople, J. A.; Binkley, J. S. Self-consistent molecular orbital methods 25. Supplementary functions for Gaussian basis sets. *J. Chem. Phys.* **1984**, *80*, 3265−3269.

(57) Khan, A. Ab initio studies of (H2O)20H+ and (H2O)21H+ prismic, fused cubic and dodecahedral clusters: can H3O+ ion remain in cage cavity? *Chem. Phys. Lett.* **2000**, *319*, 440−450.

(58) Wu, C.-C.; Lin, C.-K.; Chang, H.-C.; Jiang, J.-C.; Kuo, J.-L.; Klein, M. L. Protonated clathrate cages enclosing neutral water molecules: H+-(H2O)21 and H+(H2O)28. *J. Chem. Phys.* **2005**, *122*, 074315.

(59) Blom, C. E.; Atltona, C. Application of self-consistent-field ab initio calculations to organic molecules. II. Scale factor method for the calculations of vibrational frequencies from ab initio force constants: ethane, propane and cyclopropane. *Mol. Phys.* **1976**, *31*, 1377−1391.